

3D Effect of Ferromagnetic Materials on Alpha Particle Power Loads on First Wall Structures and Equilibrium on ITER

K. Shinohara 1), T. Kurki-Suonio 2), D. Spong 3), O. Asunta 2), K. Tani 1), E. Strumberger 4), S. Briguglio 5), S. Günter 4), T. Koskela 2), G. Kramer 6), S. Putvinski 7), K. Hamamatsu 1), ITPA Topical Group on Energetic Particles

1) Japan Atomic Energy Agency, Naka, Ibaraki, Japan

2) Aalto university, Assn. Euratom-Tekes, P.O. Box 4100, FI-02015 Aalto, Finland

3) Oak Ridge National Laboratory, Fusion Energy Theory Group, Oak Ridge, USA

4) Max-Planck-Institut-für-Plasmaphysik, EURATOM-Association, Garching, Germany

5) ENEA, Frascati, Italy

6) Princeton Plasma Physics Laboratory, Princeton University, USA

7) ITER Organization, Route de Vinon sur Verdon, F-13115 St Paul lez Durance, France

E-mail contact of main author: shinohara.koji@jaea.go.jp

Abstract. Within the ITPA Topical Group on Energetic Particles, we have investigated the impact that various mechanisms breaking the tokamak axisymmetry can have on the fusion alpha particle confinement in ITER as well as on the wall power loads due to these alphas. In addition to the well known TF ripple, the 3D effect of ferromagnetic materials and ELM mitigation coils are included in these mechanism. First, the validity of using a 2D equilibrium was investigated: a 3D equilibrium was reconstructed using the VMEC code, and it was verified that no 3D equilibrium reconstruction is needed but it is sufficient to add the vacuum field perturbations onto an axisymmetric equilibrium. Then the alpha particle confinement was studied using two independent codes, ASCOT, and F3D OFMC, all of which assume MHD quiescent background plasma and no anomalous diffusion. The distribution of the peak power load was found to depend on the first wall shape. We also made the first attempt to accommodate the effect of fast ion related MHD on the wall loads in ITER using the HMGC and ASCOT codes. The power flux to the wall was found to increase due to the redistribution of fast ion by the MHD. Furthermore, the effect of the ELM mitigation field on the fast ion confinement was addressed by simulating NBI ions with the F3D OFMC code. The loss power fraction of NBI ions was found to increase from 0.3 % without the ELM mitigation field to 5-6% with the ELM mitigation field.

1. Introduction

The new physics introduced by ITER operation, of which there is very little prior experience, is related to the very energetic (3.5 MeV) alpha particles produced in large quantities in fusion reactions. These particles not only constitute a massive energy source inside the plasma, but they also present a potential hazard to the material structures that provide the containment of the burning plasma. The assessment of the behaviour of alpha particles is one of most important activities in our group, the ITPA Topical Group on Energetic Particles.

In most theoretical approaches, the tokamak magnetic field is assumed axisymmetric. However, in reality, this symmetry is broken. As is well known, the finite number and limited toroidal extent of the Toroidal Field (TF) coils cause a periodic variation of the toroidal field called the magnetic ripple. This ripple can provide a significant channel for fast particle leakage, leading to very localized power loads on the plasma-facing components. Because of this, Ferromagnetic Inserts (FIs) will be embedded in the double wall structure of the ITER vacuum vessel in order to reduce the ripple[1]. In ITER, the toroidal field perturbations are further locally enhanced by the presence of discrete ferromagnetic structures, the Test Blanket Modules (TBM). Thus, there are complex symmetry-breakings in ITER. It is not yet theoretically understood how complex symmetry-breakings affect the fast ion confinement

and concerns have been voiced that the symmetry-breakings might introduce new, unexpected channeling mechanisms for fast ions.

Preliminary studies on alpha particle confinement have been carried out by using a variety of 5D Monte Carlo guiding-center codes: OFMC[2], [5], HYBRID[3], [4], [5], ASCOT[6], [7], DELTA5D[8], and an upgraded version of OFMC, F3D OFMC code[11], [12], [13]. In fact, the results of Ref [5] by OFMC and HYBRID codes revealed the importance of the reduction of TF ripple in ITER, and the installation of FI was proposed. Also the full orbit-following code, SPIRAL[9], has been used for confinement studies, while preliminary results for the power loads on ITER wall structures were obtained using ASCOT[7].

All these simulations were carried out using data that has later been either changed (the wall structure and geometry of FIs) or found deficient (the 3D magnetic background corresponding to the situation with TBMs). In this work, the wall power loads due to fusion-born alpha particles are re-studied for a variety of cases addressing issues such as different wall configurations, proper inclusion of the TBM effect on the magnetic background, and the possible corrections to 3D equilibrium introduced by the ferromagnetic materials. The latter is accomplished using the full free boundary 3D equilibrium code, VMEC[10], while to properly include the TBM effect on the magnetic background, the FEMAG code [11] is applied. Whereas in the past the effect of the ferromagnetic materials was calculated on the vacuum field only, in FEMAG the effect is calculated on the total field including the poloidal field due to the plasma current as well as the vacuum field. We also study the effect of the ELM mitigation coils on fast ion confinement, and attempt to assess the effect of fast ion related MHD on alpha confinement and wall loads.

The paper is organized as follows. Section 2 presents the careful analysis of the 3D magnetic field using VMEC and FEMAG codes. In Sec. 3, the confinement of fusion alphas is investigated using two independent codes, ASCOT and F3D OFMC, and the power load on a variety of different wall shapes is evaluated. In this section also the effect of ELM mitigation coils and fast-ion related MHD are addressed. Finally, in Sec. 4, we summarize our results.

2. Construction of the 3D magnetic field

Ferromagnetic material affects the strength of the magnetic field and slightly changes its direction outside the ferromagnetic regions. Therefore, in order to properly include the effect of FIs and TBMs on the ITER magnetic field, it is not sufficient to calculate the effect on the vacuum field only. For this work, the 3D magnetic background was calculated by using the FEMAG code [11]. The FEMAG code models the ferromagnetic material as thin plates with magnetic charge on the edge. The magnetic charge is distributed according to the direction of the external magnetic field and its strength is determined by the saturated magnetization of the ferromagnetic material. The external field includes the toroidal field as well as the poloidal field due to the plasma current and poloidal coils. The input parameters, such as the geometry data of FIs, are the same as in Sec. 2.3 and 3.1 of Ref. [13]. In this paper, FI [14] and Helium-Cooled Lithium-Lead (HCLL) TBM [15], [16] are installed (as shown in

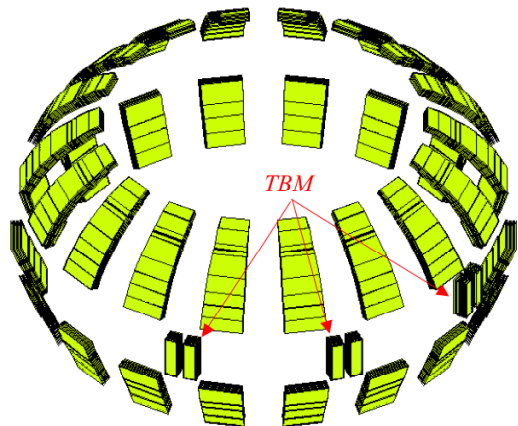


FIG. 1. FI and TBM distribution modeled in FEMAG calculation

Fig. 1). The FIs are installed keeping the 18-fold symmetry (20-degree periodicity) in the toroidal direction in this assessment.

Usually the plasma equilibrium is calculated in 2D, assuming axisymmetry. However, the 3D magnetic background/perturbation might affect the axisymmetric current. Furthermore, the resultant 3D equilibrium might induce additional symmetry-breaking. This mechanism might be enhanced through the modified plasma diamagnetic and Pfirsch-Schlüter currents when finite β effects are considered. In order to assess the significance for an ITER plasma, the 3D equilibrium was calculated using the full free boundary 3D equilibrium code, VMEC [10].

ITER plasma corresponding to Scenario 4 operation was chosen as the subject of this study. Scenario 4 is a steady state 9MA scenario with a weak negative magnetic shear, a highly shaped plasma, and a volume-averaged plasma beta of $\langle\beta\rangle = 2.24\%$, producing about 300MW of fusion power with $Q = 5$ for 3000 s [17]. Even though the power production in Scenario 4 is smaller than in a standard scenario, due to its lower plasma current the fast ion orbits are wider and, thus, fast ions in Scenario 4 plasma are more vulnerable to off-normal field configurations. The field aberration is compared between a full 3D equilibrium reconstruction and the standard case, where an axisymmetric equilibrium is augmented with the 3D vacuum fields. Two approaches were carried out for the constraint of current distribution. In the first approach, the q profile was given. In the second approach, the current profile was given. The field aberration/ripple δ is defined as $\delta = (B_{\max} - B_{\min}) / (B_{\max} + B_{\min})$, and, thus, in the absence of any TBM field bumps it reduces to the regular toroidal ripple.

With the given q -profile, the effect of the TF ripple alone was first investigated, and the β dependence of the effect was also studied [18]. The TF ripple reaches 1% at the surface of the plasma [13]. It was found that the effect of the TF ripple increased with increasing of the β -

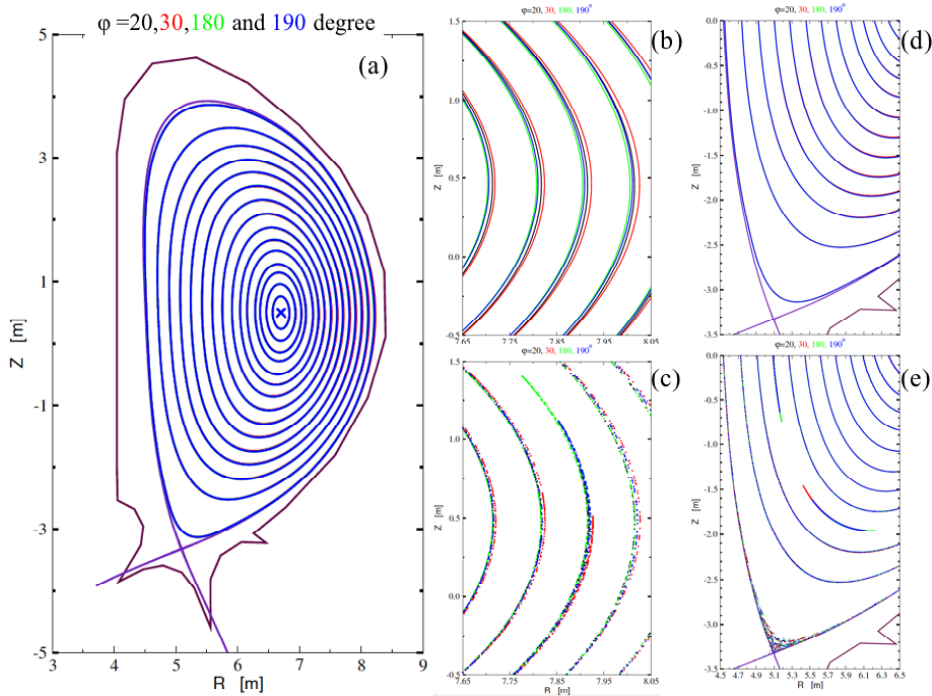


FIG. 2. The effect of the TBMs on the magnetic flux surfaces for 3D equilibrium calculations ((a), (b), (d)) and axisymmetric equilibrium + vacuum perturbation field ((c), (e)). The figures show the flux surfaces (3D calculations) or Poincaré plots of traced field lines (axisymmetric case+ perturbation) at various toroidal angles ($\phi = 20, 30, 180$ and 190 degree). (b), (c), (d) and (e) are enlargements of (a) for the midplane and the x-point regions, respectively.

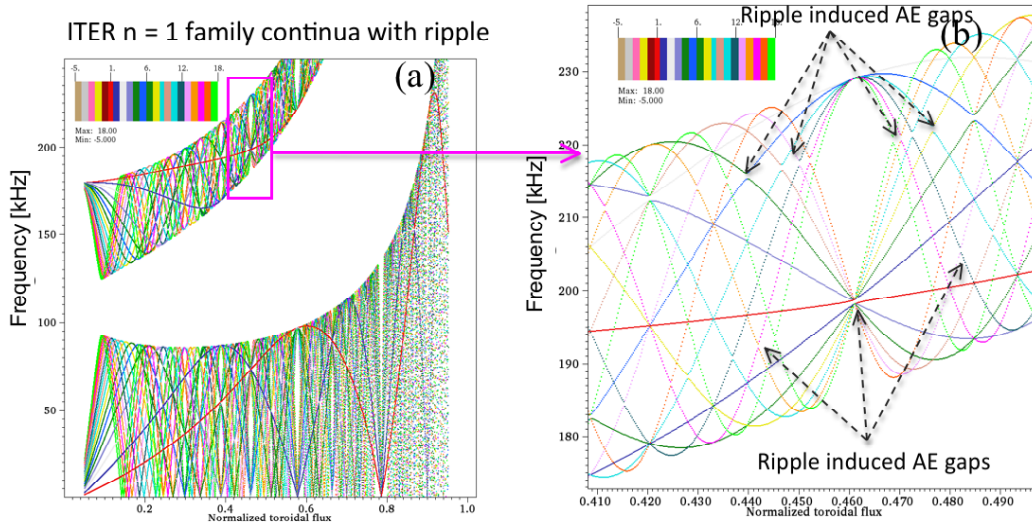


FIG. 3. $n = 1$ mode family of Alfvén continua with TF ripple, FIs and TBMs. TBM field is amplified by a factor 5 in this figure to enhance the new gap. (b) is the expanded view for the enclosed region in (a)

value, but the effect was small. The maximum difference in the ripple amplitude was about 0.05% even for the case of $\langle \beta \rangle = 4.67\%$, see Fig. 2 in Ref. [18]. When the same study was repeated for the non-axisymmetric background including the FI and TBM contributions, the β scan could not be completed. For β -values higher than $\langle \beta \rangle = 2.24\%$, the $n=1$ perturbation increased. The stability analysis with CASTOR_FLOW code [19] revealed that higher β equilibria are strongly unstable with respect to $n = 1$ ideal kink modes. Even so, the difference between the 3D equilibrium and the standard case was small as shown in Fig. 2. The similar conclusion was also obtained from the second approach.

From this study, it can be concluded that no 3D equilibrium reconstruction is needed but it is sufficient to add the vacuum field perturbations onto an axisymmetric equilibrium.

Also the structure of the Alfvén continuum was investigated for the 3D equilibrium. Figure 3 shows the $n = 1$ mode family continuum for ITER with TF ripple, FIs and TBMs. It was found that 3D field ripple couples different n 's and produces new gaps. Though its radial structure is small, it might affect the damping mechanism of the Alfvén eigenmodes.

3. Confinement of fast ions and power load on the first wall

3.1 Benchmark and the effect of different wall shapes

Under the framework of the ITPA Topical Group on Energetic Particles, we decided to simulate the fast ion confinement and power load on the first wall using two independent codes: ASCOT, and F3D OFMC codes. It was assured that both codes have identical input data that corresponds to the ITER Scenario 4 operation described above. The 3D magnetic background calculated by the FEMAG code was used including the TF ripple, the correction field by the FIs and the perturbation by TBMs. The confinement of the fusion alphas was simulated assuming only neoclassical transport via Coulomb collisions with a stationary, Maxwellian background plasma, i.e. neglecting any MHD activity or turbulent transport. For the benchmark study, axisymmetric first wall was applied.

In all the confinement simulations, the loss power fraction was found to be less than 0.2%. ASCOT and F3D OFMC codes were also used to address the question of the significance of the island structures observed in the magnetic backgrounds in the presence of the TBMs [7]. They were first discovered when the backgrounds were created with the method considering

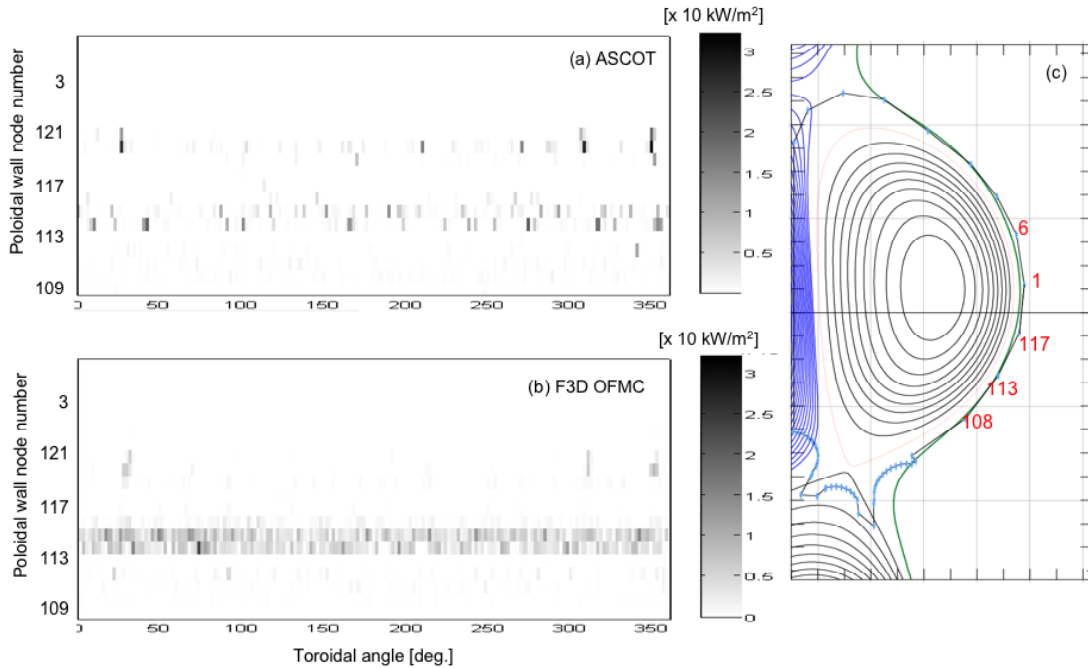


FIG. 4. Heat load distribution for: (a)ASCOT and (b)F3D OFMC. The horizontal axis is a toroidal angle which starts from TFC-1. TBMs are installed around 30, 310, and 350 degrees. The vertical axis is an poloidal wall node number as illustrated in (c).

only the contribution of the vacuum field on the TBMs. Including the plasma current contribution might reduce the island sizes, maybe eliminate them altogether. From a comparison with different background field, it was found that including the plasma current contribution in the magnetic field calculation changed the island structures only slightly and did not produce significant changes in the results.

The power loads on the first wall were also evaluated. The power load distribution is plotted in Fig. 4. The power load is less than 50 kW/m^2 . This value is well below the critical level of $\sim 1 \text{ MW/m}^2$ for this region. Thus this combination of the FI, TBM, wall shape, and plasma shape is acceptable from the material tolerance point of view. The dominant region of power load distribution is not always around the midplane of the plasma. There is a heat load distribution below the midplane, about 50 degree below in the poloidal angle. It should be noted that there is little heat load on the region in the previous work for the same 3D magnetic background, but somewhat different wall shape[13]. Thus the peak power load depends on the first wall shape. The wall shape in the previous work is the so-called limiter-like wall shape. In Fig. 5, results of F3D OFMC simulations are shown for the dependence of power load on the wall shape. The dependence on wall shape around the midplane in the low field side (LFS) was scanned. The wall shape which is labeled as W-benchmark is

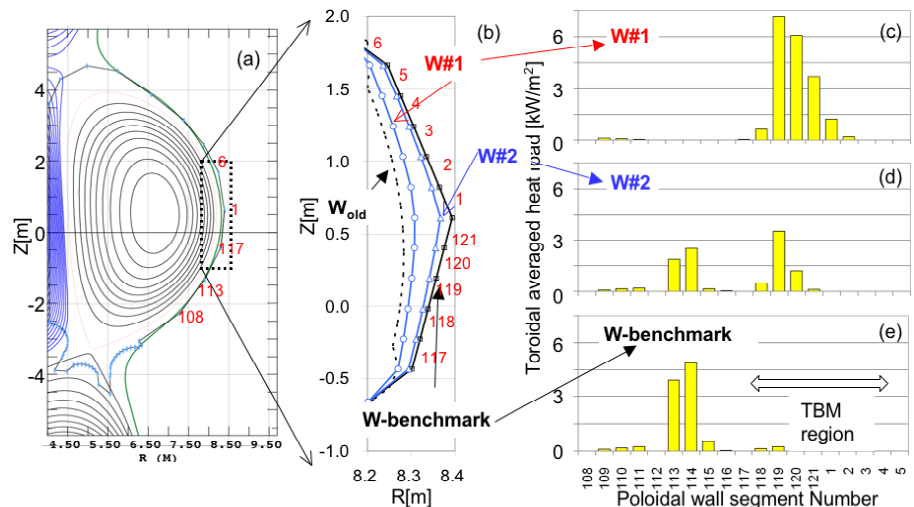


FIG. 5. Toroidally averaged poloidal distributions of heat load for various wall shapes. (a) Shape of plasma and first wall, (b) A blow-up of outer midplane region with different wall geometries, (c) Poloidal heat load distribution for wall shape W#1, (d) for W#2, (e) for W-benchmark

that in this benchmark, and the shape which is labeled as W#0 is that in the previous work in Ref. [13]. And the intermediate wall shapes, which were artificially designed for this wall shape scan, are labeled as W#1 and W#2. The peak heat load is not always at the TBM position. As the wall moves away from the plasma, heat load around the midplane decreases while heat load on the lower position increases.

ASCOT simulations also indicated that the limiter structures, located at two particular locations in toroidal angle, received much larger peak heat flux. These results from the wall study dependence indicate the importance of our continuing contribution to the re-evaluation of power loads following updates in wall shape geometry and plasma equilibrium.

3.2. Effect of MHD on the heat load

Plasmas with a large population of energetic ions might exhibit various fast ion -related MHD phenomena such as Alfvén eigenmodes. ITER, with its high fusion yield, will not be an exception. This MHD activity will act back on the energetic ions possibly transporting them towards the plasma edge, where the TF ripple and TBM field perturbation provide an efficient mechanism for moving ions to the plasma-facing components. Therefore we wanted to find a way to simulate the wall power load not only from the slowing-down distribution of the fusion alphas but also from a distribution that has been affected by the relevant MHD.

The Hybrid MHD-Gyrokinetic Code (HMGC) [20] can calculate the 4D alpha particle density in the presence of Alfvén modes. In the HMGC simulations, it was found that the $n=2$ Alfvén modes that peak around the minimum- q position can appear. The interaction of these $n=2$ Alfvén modes on the fusion alphas in the Scenario 4 plasma was evaluated [21]. The resulting alpha distribution was then used in ASCOT as input, and the simulation results were compared to a simulation in the absence of Alfvén eigenmodes. Naturally the proper way of addressing the effect of MHD activity on fast ion distribution would be to follow the test particles in the time-dependent perturbed field due to the MHD activity because wave-particle interaction is an important mechanism in this kind of transport. However, the wave-particle interaction itself, simulated in nonlinear MHD codes such as HMGC and MEGA [22] needs enormous computing resources and a comprehensive approach remains a future challenge. Therefore we had to settle for a first-order comparison of results that are obtained simply using different input profiles for ASCOT.

Normally the particle input is a source rate profile due to the fusion born alpha particles or NBI-ions. In this analysis, however, only a steady state phase space density profile was available from HMGC. The meaningful wall simulation should then consider only prompt losses since there is no way of keeping the profile stationary. Therefore the wall load was evaluated following the orbits of test particles for only 100 μ s.

The two different alpha distributions used in ASCOT wall power load simulations are dubbed “initial” and “saturated”. The name “initial” refers to distribution at the time when MHD only starts to evolve, while “saturated” corresponds to the time when MHD activity is saturated in HMGC. The population of energetic alpha particles is

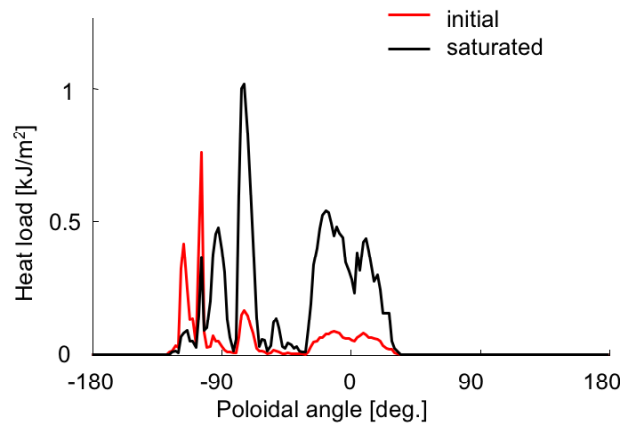


FIG. 6. Wall load for “initial” distribution and for “saturated” distribution. Poloidal angle starts at the midplane in LFS and increases in the counter-clock-wise direction.

increased at the outer region due to the redistribution by the Alfvén modes. In 100 μs , the loss energy was increased from about 15kJ in the case of “initial” distribution to about 50kJ in the case of “saturated” distribution. The power flux to the wall was found to increase. The peak power flux increased by an order of magnitude in the most serious region as shown in Fig. 6.

3.3 Effect of magnetic field by ELM mitigation coils

In order to protect and guarantee a reasonable lifetime for the divertor plates in ITER, at least the type I ELMs have to be mitigated. One way of accomplishing this is via ELM mitigation coils that change the magnetic field structure thus providing yet another symmetry-breaking mechanism for the ITER magnetic field. The design of ELM mitigation coils is also on-going in ITER. We investigated the effect of ELM mitigation field on the fast ion confinement based on the design in 2009 [23]. The coil current is configured to produce an $n=4$ perturbation, and the phase of the coil current of the upper and lower coils is shifted by -12.4 and -3.4 degrees, respectively, compared to the equatorial coil. The fields produced by the ELM mitigation coils were added to the above mentioned 3D field, which includes the TF ripple, the perturbation by FIs and TBMs. The calculation was carried out using the F3D OFMC code, and the loss power fraction of alpha particles was found to slightly increase from $\sim 0.2\%$ without the ELM mitigation field to $\sim 0.4\%$ with the ELM mitigation field. On the other hand, the loss power fraction of fast NBI deuterium ions was found to increase from $\sim 0.3\%$ without the ELM mitigation field to 5-6% with the ELM mitigation field. This level of loss power fraction might not be negligible. It is thus necessary to continue simulating the effect of the ELM mitigation field in the updated designs and other background plasmas.

4. Summary

Within the ITPA Topical Group on Energetic Particles, we have investigated the 3D effect of ferromagnetic materials and ELM mitigation coils as well as a TF ripple, i.e. complex symmetry-breaking effect in ITER.

To start with, we investigated the effect of the 3D magnetic background on the equilibrium. By the self-consistent 3D equilibrium reconstruction using the VMEC code, it was concluded that it was sufficient to add the vacuum field perturbations onto an axisymmetric 2D equilibrium on ITER in this design even with TBM perturbation, which is the largest magnetic perturbation.

The evaluation of the alpha particle confinement was carried out by using ASCOT and F3D OFMC codes. As the result, the loss power fraction was found to be less than 0.2%.

Sensitivity of the peak heat load on the first wall shape was observed. On the analysis of the F3D OFMC code, the peak heat load is not always at the TBM position when the wall shape is changed only around the midplane region. ASCOT simulations also indicated that the limiter structures received about an order of magnitude larger peak heat flux. These results for the wall shape dependence indicate the importance of the re-evaluation of power loads following updates in the wall shape and equilibrium.

An attempt to accommodate the effect of fast ion related MHD on the wall load in ITER was carried out using the ASCOT code. The heat load was compared for two fast ion profiles calculated by the HMGC code: one at the time when MHD only starts to evolve, and the other

for saturated MHD activity. The peak power flux to the wall due to direct losses was found to increase by an order of magnitude.

We also investigated the effect of the ELM mitigation coils on the fast ion confinement based on the design in 2009. The loss power fraction of NB-induced fast ions apparently increased from ~0.3 % without the ELM mitigation field to 5-6% with the ELM mitigation field. Further calculations will be done on the effect of the ELM mitigation field on fast ion confinement when the design of ELM mitigation coils is updated.

Our group will continue to contribute to the ITER design.

The views and opinions expressed herein do not necessarily reflect those of the ITER Organization

Acknowledgments

We would like to thank to Drs V. Mukovatov, T. Oikawa, S. Konovalov, J. Snipes, Y. Gribov for their encouraging our activity and providing us useful information. Part of this work was supported by the Academy of Finland Project 121371.

Reference

- [1] "Progress in the ITER Physics Basis", 'Chapter 1: Overview and summary' and 'Chapter 5: Physics of energetic ions', Nucl. Fusion **47** (2007)
- [2] Tani K., et. al., J. Phys. Soc. Jpn., **50** (1981) 1726
- [3] Konovalov S.V., et al., JAERI-Research 94-033 (1994)
- [4] Konovalov S.V., "Alpha particle ripple loss in S4 and S2 ITER reference scenarios", ITER Physics Design Task 2, RRC "Kurchatov Institute", July 20, 2001
- [5] Tobita K., et. al., Plasma Phys. Control. Fusion **45** (2003) 133
- [6] Heikkinen J. A. and Sipilä, Phys. Plasmas **2** (1995) 3724
- [7] Kurki-Suonio T., et.al., Nucl. Fusion **49** (2009) 095001
- [8] Spong D. A., et. al., Plasma Physics Reports, **23** (1997) (page 483, sect. 3)
- [9] Kramer G., et.al. "First wall heat loads and fluences from fusion-born alpha particles in ITER", 2nd meeting of the Energetic particle Topical Group, Daejeon, Korea, (2009)
- [10] Hirshman S.P. and Lee D.K. Comput. Phys. Commun. **39** (1986)161
- [11] Shinohara K., et. al., Nucl. Fusion **43** (2003) 586
- [12] Shinohara K., et.al. , Nucl. Fusion **47** (2007) 997
- [13] Shinohara K., et.al., Fusion Engineering and Design **84** (2009) 24
- [14] Morimoto M., (private communication), "Segmentation of the ferromagnetic insert", 21-Aug-2007
- [15] Rampal G., et. al., Fusion Engineering and Design **75-79**, (2005) 917
- [16] Rampal G., (private communication), HCLL TBM FM steel model_21Jun07.pdf
- [17] Polevoi A.R., et.al. 2002 Proc. 19th Int. Conf. on Fusion Energy 2002 (Lyon, 2002)
- [18] Strumberger E. et al., Nuclear Fusion **50** (2010) 025008
- [19] Strumberger E. et al Nucl. Fusion **45** (2005) 1156
- [20] Briguglio S., Zonca F., and Vlad G., Phys. Plasmas **5**, (1998) 3287
- [21] Vlad G. et al., Nucl. Fusion **46** (2006) 116.
- [22] Todo Y. and Sato T., Phys. Plasmas **5** (1998) 1321
- [23] Private communication, INTERIUM REPORT ON IMPACT OF PROPOSED "MODIFIED BASELINE" AND "ALTERNATIVE VACUUM VESSEL" DESIGNS ON ITER ELM COILS, 26-Jun-2009